DOR: 20.1001.1.27170314.2022.11.1.4.0

Research Paper

Experimental Study on In-Depth Residual Stress due to 420 Stainless Steel Creep-Feed Grinding Using the Deflection-Electro Polishing Technique

Vahid Jafarpour[1], Rasoul Moharrami[2*]

[1]Department of Mechanical and Aerospace Engineering, University of Texas at Arlington, Texas, USA

[2]Engineering Faculty, University of Zanjan, Zanjan, Iran

[*]Email of Corresponding Author: r_moharami@znu.ac.ir

Received: April 4, 2022; Accepted: May 14, 2022

Abstract

In the current study, the deflection-electro polishing method was used to evaluate through-thickness residual stresses. A modified equation was developed to calculate the non-uniform residual stresses of creep-feed ground plates concerning the three-order polynomial curve fitting of the deflection in the specimens. Employing the current density of 825 A/m^2 for the specimens caused stressed materials to be removed from their surface with the corrosion rate of 1 µ/min, which facilitated estimating the thickness of the removed layers concerning corrosion time. To investigate residual stresses created by creep-feed grinding, three different cooling conditions, i.e. dry, flood, and small quantity cooling lubrication (SQCL) were tested. The literature review showed a dearth of research on through-thickness residual stresses under SQCL creep-feed grinding. The results demonstrated that due to a considerably lower flow rate of the SQCL compared to that of the flood cooling system, considerable performance was detected so that compressive residual stresses were observed in the depth beneath the surface.

Keywords

Residual Stresses, Electro-polishing, Creep-feed Grinding, Small Quantity Cooling Lubrication

Abbreviation			
E	Young's modulus[GPa]	M	Moment [Nm]
a	Depth of cut [µm]	V_s	Wheel liner speed [m/s]
F	Force [N]	V_w	Feed rate [mm/s]
b	Width of the specimen [mm]	f_x	Deflection of the specimen [mm]
H	Thickness of the specimen [mm]	L	The length of specimen exposed to corrosion [mm]
y	Distance above from removed layer [mm]	y_0	Variable amount related to removed layer thickness [mm]
σ_{y_0}	Total residual stress in each layer beneath the surface of the specimen [MPa]		

1. Introduction

Grinding is one of the important machining processes for manufacturing industrial parts, which calls for excessive surface integrity and particular geometries. Creep-feed grinding may be taken into

consideration as small-chip or abrasive machining, able to change broaching or milling the machining of complex forms and slots, in hard-to-grind materials, such as advanced alloys and hardened tool steels. This producer goals to decrease the processing time by minimizing the grinding passes. To achieve this, the magnitude of cutting depth has expanded some orders compared to conventional grinding. As the process completes a part in one pass and a single fixturing, the creep-feed grinding decreases the total cost and time and improves efficiency.

Despite all merits of creep-feed grinding, it should be mentioned that a trade-off is always between surface imperfection and efficiency in the process. The increasing rate of material removal leads to incensement in the generation of heat and temperature because of wheel workpiece friction and plastic deformation of chips in the contact area. When heating results in excessive temperature, considerable surface changes, and subsurface damage may happen, including phase transformation, cracking, hardness changes, and unwanted residual stresses [1-2]. The heat created in the grinding area is generally eliminated by chips, the workpiece, wheel, and coolant, which vary depending on grinding parameters. Nevertheless, a workpiece exposed to process commonly reports a speedy cooling-heating cycle [3-5]. A particularly good example of this is research conducted by S. Kohli et al. [6], reporting that the amount of heat absorption into the workpiece can considerably differ depending on the type of grinding wheel. In their study one-third reduction was observed using CBN abrasive wheel instead of aluminum oxide. This is while the coolant plays a more significant role in absorbing generated heat during creep-feed grinding, reported at more than 90% [5-7].

To reach a good surface quality, controlled-stress creep-feed grinding is a necessity. For controlling stresses generated by grinding processes, elements causing them must be perceived. Relying on their kind, residual stresses are either desirable or detrimental. Mechanical plastic transformation, thermal plastic transformation, and phase transformation are three factors to generate residual stresses in the creep-feed grinding process. The first and third factors are compressive, whereas the second is tensile [8]. It should be noted that cooling conditions greatly affect the nature of residual stresses (compressive or tensile) generated in creep-feed grinding. The most unwanted and harmful tensile stresses are observed under dry grinding whereas flood grinding, depending on the kind of coolant, reduces the grinding temperature and generates desirable residual stresses [9]. Although many industries have stayed true to the conventional cooling systems, this is no longer appropriate owing to high costs, ineffective closed-loop coolant circulation, and health and environmental risks [10-12]. Nowadays, researchers have become interested in a new environmentally friendly technique, namely spraying nozzles, which atomize different coolants into the grinding area to investigate the residual stress behavior [13-15]. This environmentally friendly method can be named Minimum Quantity Lubrication (MQL) or Small Quantity Cooling Lubrication (SQCL) depending on the amount of flow rate. As a criterion, it is interesting to mention that the coolant consumption in conventional flood cooling varies from 10 l/min to 100 l/min, whereas this amount is 5-100 ml/h in MQL and up to 1000 ml/h in SQCL [16-18]. However, it should be pointed out that it is not always possible to achieve an acceptable outcome through the low amount of coolant particular in the creep-feed grinding process which the temperature history is quite high and the MQL system does not function effectively, hence the necessity for higher flow rates is felt. The SQCL method is presented as an appropriate alternative to MQL which contains a wider variety of flow rates up to a thousand ml/h.

On the other hand, designers always tend to diminish undesirable residual stresses in ground components with an appropriate choice of grinding parameters. This could be obtained best in case they have dependable data from grinding events. It is worth mentioning that as experimental data are based on reality, they can be a reliable analysis tool. However, the costs of experiments should be considered, and choosing unexpansive and highly efficient methods are of particular importance.

In this study, the deflection-electro polishing technique was selected as the residual stress measurement method. This selection was due to several merits of this method compared to others. Let us consider neutron diffraction as an example. Because of the high penetration of neutron beams into materials, unlike X-ray beams, it is possible to measure through-thickness stresses, however, the existence of a nuclear reactor is pivotal and works on a certain range of materials [19-20]. Moreover, in residual stress measurement, using strain gauges is highly common, especially in hole drilling, slitting, and contour methods. However, these gauges are disposable and require a quite long preparation and installation time [21-23]. Therefore, a method is needed, which can measure through-thickness residual stresses without using any relatively-expensive consuming tool (like strain gauges) or equipment. The deflection-electro polishing technique can strongly perform this measurement with low cost, high accuracy, and simple operation [24, 25]. However, the removal of stressed materials can be performed using mechanical machinery like a five-axis milling machine or electrochemical processes [26, 27]. The electrochemical process can be electro-etching or electro-polishing related to input current density to the workpiece [28]. The electro-polishing process uniformly removes highly thin layers from the surface of the workpiece, making the surface quality far better compared to the electro etching process [29]. To measure the deflection of the workpiece after removing stressed materials from the surface, because of the mentioned limitations of strain gauges and challenges related to the acidic environment, non-contact displacement sensors are suggested.

In this work, in-depth non-uniform residual stresses were comprehensively investigated using the deflection-electro polishing technique. The electropolishing process was employed on 420 stainless steel to uniformly remove layers from the surface. Moreover, a semi-empirical equation was presented to calculate residual stress in thin creep-feed ground plates in terms of the deflection of the specimen. Notably, the literature review demonstrated a dearth of research on through-thickness residual stress behavior in the creep-feed grinding process through the SQCL cooling system. Therefore, the experiments were performed under dry, flood and small quantity cooling lubrication (SQCL) cooling conditions.

2. The deflection-electro polishing technique theory

The deflection-electro polishing technique is a destructive technique based on mechanical stress relieving to measure non-uniform residual stresses. As shown in Figure 1, the specimen is assumed to be thin and parallelepiped, stresses along the thickness are zero, and the main stress is parallel with the axis of the sample. If the layers of the material containing residual stresses are removed, the balance between internal forces and moments is disrupted at the same time, and the specimen is subjected to the following forces and moments:

$$dF = -\sigma_{y_0} b \, dy_0 \quad (1)$$

$$dM = -\sigma_{y_0} b\, dy_0 \frac{(H - y_0)}{2} \quad (2)$$

By removing a layer, the specimen is deformed which requires the opposite force dF′ and the opposite moment dM′ to rebalance it. Deformation generally depends on the type and magnitude of residual stresses.

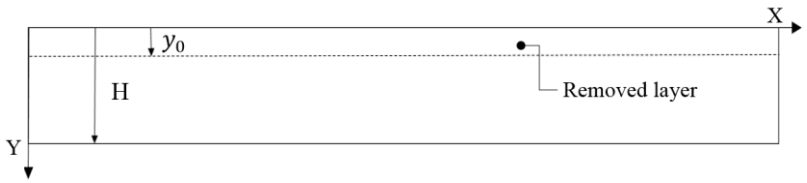

Figure 1. The schematic representation of the method

In a simply supported beam, the bending moment caused by stresses in the specimen can be obtained by the following relation:

$$M = -\frac{8EI}{L^2} f_x \quad (3)$$

According to the above relation and the moment caused by residual stresses in the specimen, variation in the deformation df_x caused by removing a layer of thickness dy_0 is expressed with the surface stress σ'_{y_0}, which is obtained by the following equation:

$$\sigma'_{y_0} = -\frac{4}{3} E \frac{(H - y_0)^2}{L^2} \frac{df_x(y_0)}{dy_0} \quad (4)$$

To obtain stress, in addition to calculating stresses in each layer, the effects of layer removal on the stress variations $\Delta\sigma$ should also be considered. The opposite force dF′ and the opposite moment dM′ cause $\Delta\sigma$ at the dimension of (H-y) so that:

$$d\sigma = d\sigma_n + d\sigma_f \quad (5)$$

$d\sigma_n$ and $d\sigma_f$ due to normal and bending stresses are given by:

$$d\sigma_n = \frac{dF'}{b(H - y)} = -\frac{4}{3} E \frac{(H - y_0)}{L^2} df_x(y) \quad (6)$$

$$d\sigma_f = dM \frac{(H - y_0) - \frac{(H-y)}{2}}{b\frac{(H-y)^3}{12}} == -\frac{8E}{L^2}((H - y_0) - \frac{1}{2}(H - y))df_x(y) \quad (7)$$

Therefore:

$$d\sigma_n = \frac{8}{3}\frac{E}{L^2}((H - y)df_x(y) - (H - y_0)df_x(y)) \quad (8)$$

The total stress variation at the dimension of (H-y) on the account of layer removal above the dimension of (H-y) is given by Equation (9):

$$\Delta\sigma = -\frac{8E(H - y_0)}{L^2}\int_0^{(H-y_0)} df + \frac{8}{3}\frac{E}{L^2}\int_0^{(H-y_0)} (H - y)df_x(y) \quad (9)$$

Finally, the amount of residual stress in the specimen for each layer is obtained from the equation below:

$$\sigma_{y_0} = \Delta\sigma + \sigma'_{y_0} \tag{10}$$

$$= -\frac{4}{3}\frac{E}{L^2}\left[(H - y_0)^2 \frac{df_x(y_0)}{dy_0} - 4(H - y_0)f_x(y_0) - 2(3y_0 - 2H)f_x(0) + 2\int_0^{y_0} f_x(y)dy\right]$$

3. Experimental

3.1 Creep-feed grinding process and Material

The material utilized in the present work is 420 stainless steel. Specimens were cut off from a stainless steel plate with 95 mm, 15 mm, and 2.15 mm (the length, width, and thickness), respectively. Before grinding, the initial stresses of specimens were relieved at 400 °C for 90 min. To measure the mechanical properties of 420 stainless steel, specimens were prepared based on E8/E8M-13a (standard test method for tension testing of metallic materials). To achieve this, the universal test machine STM-250 was employed as shown in Figure 2(a). The chemical composition of 420 stainless steel was measured based on ASTM E1010 (standard test methods for low alloy steel) using an ARUN technology PolySpec machine as demonstrated in Figure 2(b). It should be noted that to achieve reliability, each test was done three times, and their averages were utilized for data processing. The chemical composition and mechanical properties of the incorporated material after preparation are demonstrated in Table 1 and Table 2, respectively. The creep-feed grinding process was done using the MST300 grinding machine with 87 kW spindle motor power. Aluminum oxide grinding wheel with dimensions of 230 mm, 32 mm, and 76.2mm (diameter, thickness, and hole size, respectively) and specifications 96A46M9V were employed at the liner speed of 23 m/s. A single-point diamond dresser was utilized to dress the grinding wheel after each test. Each experiment was repeated three times to reach reliability, and their mean values were utilized for the analysis.

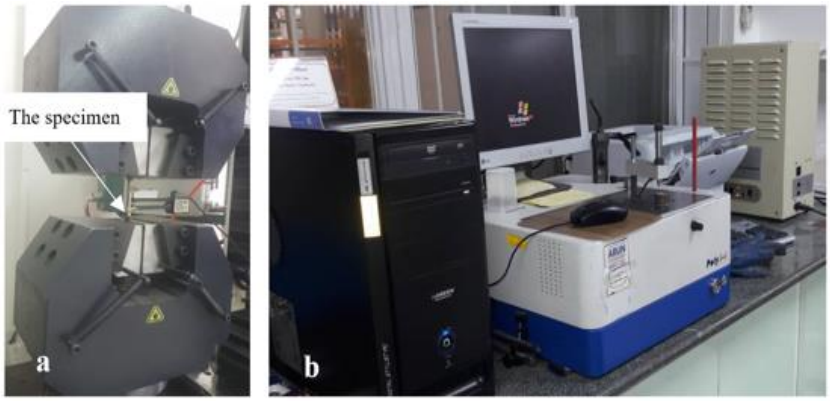

Figure 2. a) The universal test machine STM-250 b) The ARUN technology Poly Spec machine

The process was done in a pass in a grinding direction. The creep-feed grinding set-up is depicted in Figure 3. The specimens were constrained on a steel plate connected to a dynamometer, which sent the creep-feed grinding measured forces to the monitoring system. To atomize the compressed air and coolant to the grinding zone, the SQCL system was employed. As shown in Figure 3 a positive fluid flow was created via a gravity-feed container. The SQCL atomizer nozzle was stabilized at a

distance of 80 mm and an angle of 10° relative to the specimen. The air pressure and the flow rate were fixed at 6.5 bar and 400 ml/h, respectively. It should be noted that the flow rate of the SQCL system decreased about 325 times compared to that of the conventional cooling system. Figure 4 illustrates a close view of spraying the coolant into the grinding area.

Table 1.The chemical composition (wt. %) of 420 stainless steel*

Element	C	Mn	Si	Cr	Ni	Fe	Cu	P	S	V	Mo
Component (%)	0.215	0.434	0.362	12.01	0.485	86	0.165	0.023	0.005	0.036	0.084

*Measured by authors

Table 2.The mechanical properties of AISI 420 stainless steel*

Alloy Nominal Composition	Tensile Strength, Yield (MPa)	Tensile Strength, Ultimate (MPa)	Modulus of Elasticity (GPa)
AISI 420	852	920	200

*Measured by authors

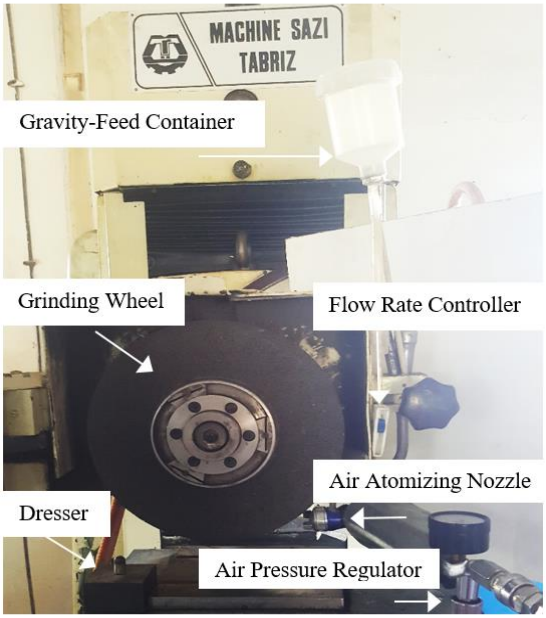

Figure 3. The creep-feed grinding set-up

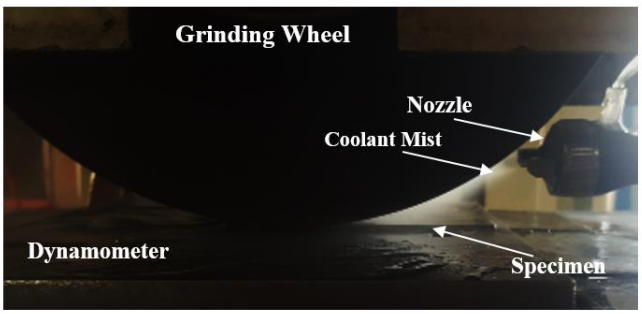

Figure 4. A view of coolant mist spray in SQCL creep-feed grinding

To investigate through-thickness residual stresses in this process, three test conditions were selected. The experiments were done under three different cooling conditions, i.e. dry, flood and SQCL. The dry and flood creep-feed grinding conditions were selected because of the creation of detrimental tensile stresses and desirable compressive stresses in the specimen, respectively. This is while the residual stress of creep-feed ground plates under the SQCL cooling system has not been yet studied. The process conditions are demonstrated in Table 3.

Table 3. The creep-feed grinding experimental conditions

Grinding machine	MST300
Mode	Surface down grinding
Specification of grinding wheel	Aluminum oxide (96A46M9V)
Dimension of grinding wheel	230 mm,32 mm, and76.2 mm(Diameter, thickness, and hole size)
Wheel speed V_s (m/s)	23
Grinding coolant	Soluble cutting oil Behran Oil Company (5vol %)
Specimen material	420 Stainless steel
Dimensions of specimen	90 mm,15 mm, and 2.15 mm(diameter, thickness, and hole size)
Environment(coolant-lubricant)	Dry, SQCL, and Flood
Flood lubrication flow rate (L/h)	130
SQCL flow rate(ml/h)	400
SQCL air pressure(bar)	6.5
Cutting depth a (µm)	150
Feed rate V_w (mm/s)	1
Dresser	Single point dresser
Total dressing depth(µm)	90
Speed of dressing(mm/s)	8

3.2. Residual stresses Measurement

Residual stresses were evaluated using the deflection-electro polishing method. As shown in Figure 5 the FASTUS CD22-100AM122 laser displacement sensor was used for measuring the deflection of the specimen constantly. Moreover, as shown in Figure 6, the measuring arm provided a condition, in which the deflection of the specimen was measured at a safe distance from the acidic environment with a 20x magnification. It should be noted that only an area of 55 mm from the grounded surface was subjected to corrosion and the remaining area was preserved by the electrical tape.

Figure 5. Layer removal setup and measuring the deflection of the specimen using the laser displacement sensor

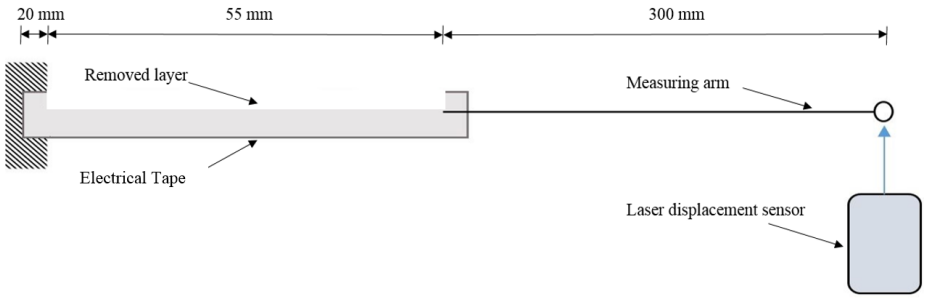

Figure 6. The schematic illustration of deflection measurement

The illustration of the measurement system is demonstrated in Figure 7. One of the challenges of using electrochemical processes is to control corrosion. Electrochemical polishing provides uniform corrosion in a way that the surface quality of the specimen becomes far better after the process compared to other chemical processes. To reach a condition similar to the theory of this method (from the uniform material removal viewpoint), the current density of 825 (A/m^2) was applied to the specimen parallel to the cathode (316 stainless steel) with a 20 mm gap. It should be noted that the surface area of the cathode must be greater than that of the anode (4:1, in this study) and the cathode must have a good surface quality. The electrolyte used in this study consists of 10 mL of HCL, 5 mL of HNO_3, and 85 mL of ethanol (95%). To stabilize the process, the electrolyte temperature should be fixed at 25 °C. Table 4 summarizes the process.

Table 4. Summary of the electro-polishing process

Electrolyte	10 ml HCL+5 ml HNO_3+ 85 ml ethanol (95%)
Cathode material	316 stainless steel
Anode material	420 stainless steel
The ratio of the area of the cathode to the anode	4 to 1
The temperature of the electrolyte (°C)	25
Current density(A/m^2)	825
The distance between the anode and cathode (mm)	20

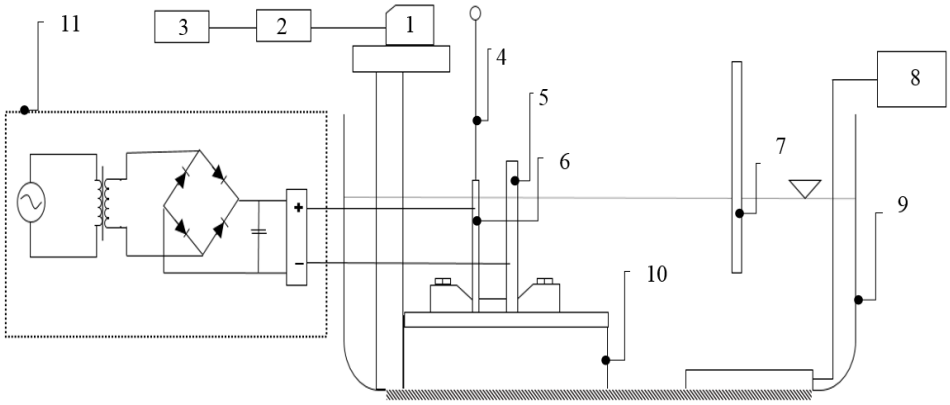

Figure 7. The scheme of a through-thickness residual stress measurement system based on the deflection-electro polishing technique 1: Laser displacement sensor, 2: Data logger, 3: Computer, 4: Measuring arm, 5: Cathode, 6: Specimen (anode), 7: Thermometer, 8: Cooling and stabilizing system, 9: Container, 10: Holder, 11: Power supply system

4. Results and discussion

As mentioned in the previous section, the electro-polishing process uniformly removes layers from the specimen surface. The relationship between corrosion time and thickness of the removed layer is demonstrated in Figure 8. As can be observed, there is a linear relationship between the thickness of the removed layer and corrosion time so the material removal rate was obtained at 1 μm/min. The controlled corrosion rate during this study facilitated the estimation of the thickness of the removed layers about corrosion time. The discreet measurements of the thickness of the specimens verified these estimations. The deflections of specimens versus the removed layer thickness under the electro-polishing process are illustrated in Figure 9. To calculate the residual stresses, it is essential to express the deflection values in terms of polynomials equations. It should be noted that the extracted equations must have the most coincidence with experimental data. In this study, the three-order polynomial equation met the needs. Therefore, the deflection of the specimen (f_x) concerning the removed layer (y_0) is presented by the following equation:

$$f_x\,(y_0) = a_1 {y_0}^3 + a_2 {y_0}^2 + a_3 y_0 + c \qquad (11)$$

In which,a_1, a_2, a_3, and c are the constant coefficients obtained experimentally. Table 5 indicates the coefficients of third-order polynomial under the dry, flood, and SQCL creep-feed grinding conditions. The coefficient of determination (R^2) is also presented for polynomial equations.

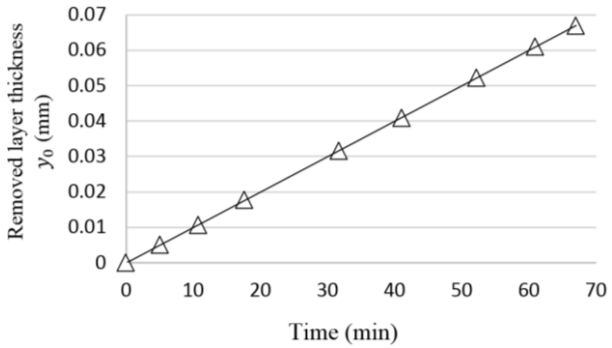

Figure 8. The material removal rate under the electro-polishing process

Table 5. The coefficients of the curve fitting

	a_1	a_2	a_3	C	R^2
DRY	-135.83	+ 32.69	+ 2.672	+ 0.0009	0.9994
FLOOD	+ 125.24	- 21.050	+ 1.1702	- 0.0006	0.9958
SQCL	+ 92.781	- 14.763	+ 0.7282	- 0.001	0.9881

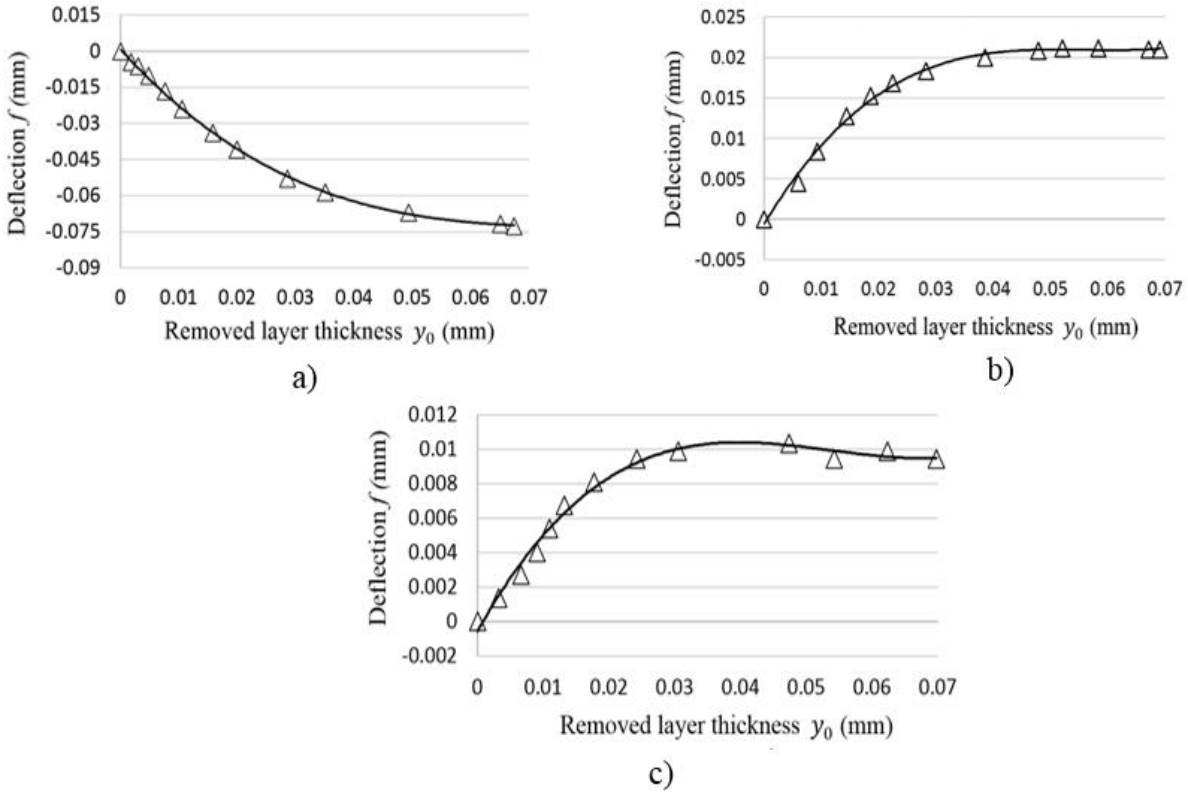

Figure 9. The measured deflections under the electropolishing process: a)dry b)flood c)SQCL

Substituting equation (11) into equation (10) resulted in:

$$\sigma_{y_0} = -\frac{4}{3}\frac{E}{L^2}\left[(H - y_0)^2(3a_1{y_0}^2 + 2a_2y_0 + a_3) - 4(H - y_0)(a_1{y_0}^3 + a_2{y_0}^2 + a_3y_0 + c) + 2\int_0^{y_0}(a_1y^3 + a_2y^2 + a_3y + c)dy\right] \quad (12)$$

The above equation calculates the through-thickness residual stress in the creep-feed grinding process. As mentioned, the deflection of the specimen is a third-order polynomial, in which a_1, a_2, a_3, and c are the constant coefficients obtained experimentally from the curve fitting. The equations of residual stress under the dry, flood, and SQCL creep-feed grinding conditions are respectively as follows:

$$\sigma_{y_0} = -0.085951\ e3\left[(2 - y_0)^2(-407.49{y_0}^2 + 65.38y_0 - 2.672) - 4(2 - y_0)(-135.83{y_0}^3 + 32.69{y_0}^2 - 2.672y_0 + 0.0009) + 2\int_0^{y_0}(-135.83y^3 + 32.69y^2 - 2.672y + 0.0009)dy\right] \quad (13)$$

$$\sigma_{y_0} = -0.085951\ e3\left[(2 - y_0)^2(375.72{y_0}^2 - 42.104y_0 + 1.1702) - 4(2 - y_0)(125.24{y_0}^3 - 21.052{y_0}^2 + 1.1702y_0 - 0.0006) + 2\int_0^{y_0}(125.24y^3 - 21.052y^2 + 1.1702y - 0.0006)dy\right] \quad (14)$$

$$\sigma_{y_0} = -0.085951\ e3\left[(2 - y_0)^2(278.343{y_0}^2 - 29.526y_0 + 0.7282) - 4(2 - y_0)(92.781{y_0}^3 - 14.763{y_0}^2 + 0.7282y_0 - 0.001) + 2\int_0^{y_0}(92.781y^3 - 14.763y^2 + 0.7282y - 0.001)dy\right] \quad (15)$$

Substituting the thickness of the removed layers into the above equations (13-15) results in through-thickness residual stress profiles, which is one of the strong points of the deflection-electro polishing technique compared to others. The non-uniform residual stress profiles under the dry, flood and SQCL cooling conditions are depicted in Figure 10. As expected from the graphs in Figure 9, the higher deflection levels are demonstrative of higher degrees of residual stress so the dry grinding condition with the maximum deflection of 0.0674 (mm) showed the maximum stress of 919 MPa at the grounded surface. This is while the flood and SQCL grinding conditions presented the maximum surface stresses of - 402 MPa and -251 MPa under the maximum deflections of 0.0210 (mm) and 0.0094 (mm), respectively. It is considered that in addition to the deflection magnitude, its direction is also important. As observed, the negative degrees of the deflection caused tensile stresses to dominate whereas the positive degrees of deflection led to desirable compressive stresses in the specimen. Moreover, it was detected that after a certain material removal rate, the deflection of the specimen was elevated gradually. After y_0= 0.04942 (mm), the specimen deflected only 0.0055 (mm) (12.18% of the total deflection) under the dry grinding condition, where the residual stress profile showed that stresses approached zero. The same conditions occurred in the flood and SQCL creep-feed grinding conditions after y_0= 0.03861 mm and y_0= 0.0305 mm, respectively.

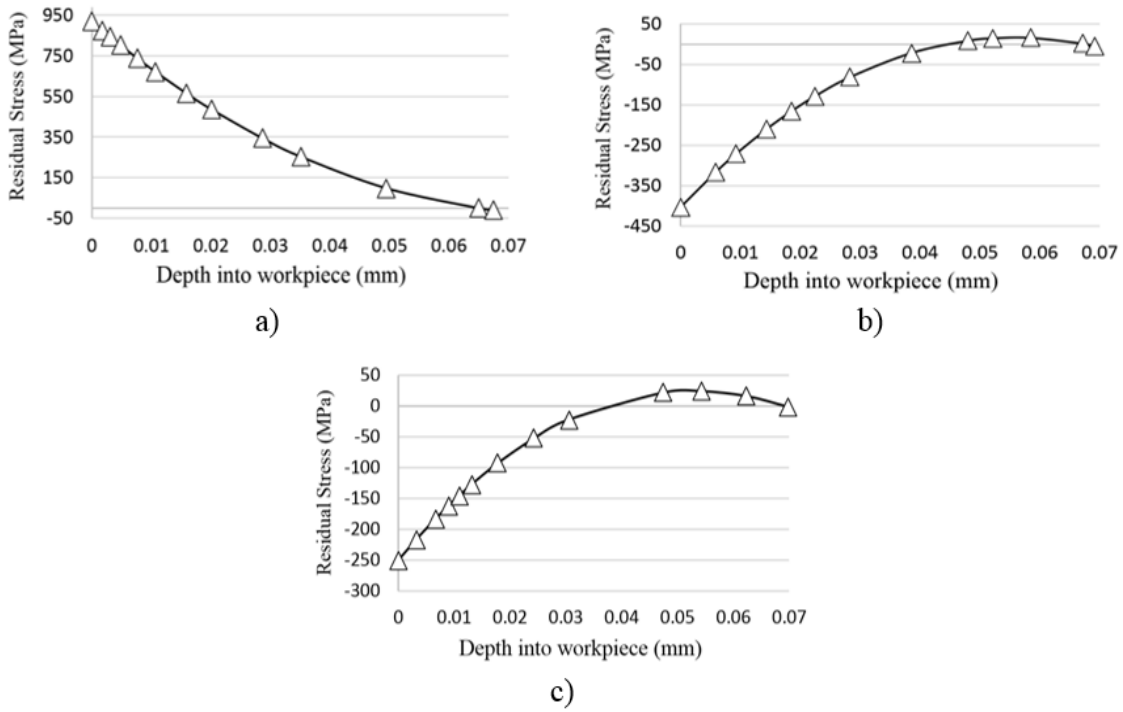

Figure 10. The values of residual stresses along with the depth of the specimen under creep-feed grinding in the a) dry, b) flood and c) SQCL conditions

The detrimental and unwanted tensile residual stresses of the dry grinding condition, observed all over the removed layers, were transformed into compressive and desirable stresses using the flood and SQCL cooling systems. However, the flood cooling system is no longer appropriate for green manufacturing. Chief among the drawbacks of flood cooling system is that coolant consumption is quite high, in this study 130,000 ml/h, whereas the flow rate of SQCL cooling system is by far lesser, in this study 400 ml/h (325 times lower). This high amount of flow rate can result in health and environmental problems. Further, the costs of recycling or disposal of coolants are exorbitant and include a lot of total machining costs, hence considerable reduction in consumption of coolants in the SQCL cooling system is of great merit. Therefore, the SQCL can be an interesting alternative method for conventional flood cooling with enhanced cooling and heat dissipation ability, in that cooling is done by atomizing the small amount of coolant using compressed air on the grinding zone. A glance at Figure 9 also reveals some striking similarities between Flood and SQCL cooling systems. Both systems provided dominant compressive residual stresses throughout the removed layers. The highest degree of compressive stress under flood cooling conditions was obtained near the surface with a magnitude of 402 MPa. The following 20 micrometers (from the surface) saw a rapid decline in the residual stresses, to somewhere in the vicinity of 150 percent. It was followed by a sustained fall, with compressive stresses in the specimen, reaching the lowest point of zero in the depth of 70 micrometers. The highest value of compressive stress under the SQCL cooling system, meanwhile, was observed close to the top side with a magnitude of 251 MPa (60 percent reduction compared to that of flood). These stresses, then plunged to a low of -50 MPa in the depth of 25 micrometers, followed by a steady decline. It is interesting to note that the SQCL cooling condition indicated a close performance to that of the flood cooling system regardless of any differences to flow rates in

terms of the residual stresses behavior. However, the residual stresses in the creep-feed grinding process are a result of a complicated mechanism. In particular, the performance of SQCL cooling condition depends on a wide range of spraying parameters including the nozzle direction, air pressure, the distance toward the grinding contact zone, flow rate, spring cone angle, and so on, which can play a significant role in generating compressive residual stresses even better than that of the flood.

5. Conclusion

High tensile and compressive residual stresses were generated by the creep-feed grinding process. To some extent generating these detrimental or desirable stresses depend on the type of cooling system. Primarily based on the results of the current experimental study, the subsequent conclusions may be drawn:

- Tensile stresses were observed throughout the thickness of the specimen under dry grinding, reaching a peak of 919 MPa near the surface, followed by a steady decline.
- Compressive residual stresses, then, were observed in the specimens through the flood and SQCL cooling conditions. The maximum values were obtained close to the surface with a magnitude of 420 MPa and 251 MPa under flood and SQCL cooling systems, respectively.
- Similar residual stress behavior between two cooling systems (flood and SQCL) was observed while the cooling consumption saw a drastic decrease of 325 percent in the SQCL system. Therefore, given the problems of flood cooling systems, the SQCL cooling condition can be an interesting alternative. However, it should be noted that the spraying parameters of this study were fixed and only the through-thickness residual stresses behavior was investigated. The authors suggest that to achieve a closer residual behavior or even a better one, other spraying parameters should be investigated.
- A novel semi-empirical equation was proposed to calculate residual stresses. In this equation, a shape function was developed, representing variation in deflection of the specimens concerning removal depth. The proposed function was founded as a three-order polynomial, with constant coefficients, which are obtained experimentally. Results have shown that relying on the direction and magnitude of the released stresses, these coefficients varied. Consequently, the residual stresses distribution pattern can differ, depending on cooling conditions.

6. Acknowledgment

The authors desire to thank the members of the Analysis, Measurement, and Engineering of Residual Stress (AMERS) Research Lab for their constant technical support in this investigation.

7. References

[1] Kim, H.J., Kim, N.K. and Kwak, J.S. 2006. Heat Flux Distribution Model by Sequential Algorithm of Inverse Heat Transfer for Determining Workpiece Temperature in Creep Feed Grinding. International Journal of Machine Tools and Manufacture. 46(15): 2086–2093.

[2] Jin, T. and Stephenson, D.J. 2003. Investigation of the Heat Partitioning in High-Efficiency Deep Grinding. International Journal of Machine Tools and Manufacture. 43(11):1129–1134.

[3] Lavisse, B., Lefebvre, A., Torrance, A.A., Sinot, O., Henrion, E., Lemarié, S. and Tidu, A. 2018. The Effects of the Flow Rate and Speed of Lubricoolant Jets on Heat Transfer in the Contact Zone when Grinding a Nitrided Steel. Journal of Manufacturing Processes. 35: 233-243.

[4] Jamshidi, H. and Budak, E. 2018. Grinding Temperature Modeling Based on a Time Dependent Heat Source. 8th CIRP Conference on High Performance Cutting. Procedia CIRP. 77: 299–302.

[5] Jin, T. and Stephenson, D.J. 2006. Heat Flux Distributions and Convective Heat Transfer in Deep Grinding. International Journal of Machine Tools and Manufacture. 46(14):1862–1868.

[6] Kohli, S., Guo, C. and Malkin, S. 1995. Energy Partition to the Workpiece for Grinding with Aluminum Oxide and CBN Abrasive Wheels. Journal of Engineering for Industry.117 (2): 160-168.

[7] Jafarpour, V. and Moharrami, R. 2022. Numerical Stress Analysis of Creep-Feed Grinding Through Finite Element Method in Inconel Alloy X-750. Mapta Journal of Mechanical and Industrial Engineering (MJMIE). 6(1): 1–9.

[8] Liu, M., Nguyen, T., Zhang, L., Wu and Q., Sun, D. 2015. Effect of Grinding-induced Cyclic Heating on the Hardened Layer Generation in the Plunge Grinding of a Cylindrical Component. International Journal of Machine Tools and Manufacture. 89: 55–63.

[9] Ding, W., Zhang, L., Li, Z., Zhu, Y., Su, H. and Xu, J. 2017. Review on Grinding-induced Residual Stresses in Metallic Materials. The International Journal of Advanced Manufacturing Technology. 88: 2939–2968.

[10] Cearsolo, X., Cabanes, I., Sanchez, J.A., Pombo, I. and Portillo, E. 2016. Dry-dressing for Ecological Grinding. Journal of Cleaner Production. 135: 633-643.

[11] Saberi, A., Rahimi, A.R., Parsa, H., Ashrafijou, M. and Rabiei, F. 2016. Improvement of Surface Grinding Process Performance of CK45 Soft Steel by Minimum Quantity Lubrication (MQL) Technique Using Compressed Cold Air Jet from Vortex Tube. Journal of Cleaner Production. 131: 728-738.

[12] Sinha, M. K., Madarkar, R., Ghosh, S. and Rao, P. V. 2017. Application of Eco-friendly Nanofluids during Grinding of Inconel 718 through Small Quantity Lubrication. Journal of Cleaner Production. 141:1359-1375.

[13] Verma, N., Kumar, M. K. and Ghosh, A. 2017. Characteristics of Aerosol Produced by an Internal-mix Nozzle and its Influence on Force, Residual Stress and Surface Finish in SQCL Grinding. Journal of Materials Processing Technology. 240: 223–232.

[14] Sai, S. S., Kumar, K. M. and Ghosh, A. 2015. Assessment of Spray Quality from an External Mix Nozzle and its Impact on SQL Grinding Performance. International Journal of Machine Tools and Manufacture. 89: 132–141.

[15] Paul, S. and Ghosh, A. 2017. Suitability of Aqueous MoS2 Nanofluid for Small Quantity Cooling Lubrication–assisted Diamond Grinding of WC-Co Cermets. Proceedings of the Institution of Mechanical Engineers. Part B: Journal of Engineering Manufacture. 233(2): 426-442.

[16] Debnath, S., Reddy, M.M. and Yi, Q.S. 2014. Environmental Friendly Cutting Fluids and Cooling Techniques in Machining: A Review. Journal of Cleaner Production. 83: 33-47.

[17] Kumar, M. K. and Ghosh, A. 2015. Synthesis of MWCNT Nanofluid and Evaluation of its Potential besides Soluble Oil as Micro Cooling-lubrication Medium in SQL Grinding. The International Journal of Advanced Manufacturing Technology. 77: 1955–1964.

[18] Roy, S., Ghosh, A. 2013. High-Speed Turning of AISI 4140 Steel using Nanofluid through Twin Jet SQL System. Proceedings of the ASME International Manufacturing Science and Engineering Conference. 2: 1067.

[19] Woo, W., An, G. B., Em, V. T., De Wald, A. T. and Hill, M. R. 2015. Through thickness Distributions of Residual Stresses in an 80 mm Thick Weld using Neutron Diffraction and Contour Method. Journal of Materials Science. 50(2): 784–793.

[20] Schajer, G. S. 2013. Practical Residual Stress Measurement Methods. John Wiley and Sons.

[21] Harrington, J. S. and Schajer, G. S. 2017. Measurement of Structural Stresses by Hole-drilling and DIC. Experimental Mechanics. 57: 559–567.

[22] Al-Mosawe, A., Agha, H., Al-Hadeethi, L. and Al-Mahaidi, R. 2018. Efficiency of Image Correlation Photogrammetry Technique in Measuring Strain. Australian Journal of Structural Engineering. 19(3): 2204-2261.

[23] Schajer, G.S. and Whitehead, P. S. 2017. Hole-drilling Method for Measuring Residual Stresses. Morgan and Claypool Publishers.

[24] Rossini, N.S., Dassisti, M., Benyounis, K.Y. and Olabi, A.G. 2012. Methods of measuring Residual Stresses in Components. Materials and Design. 35: 72–588.

[25] Moharrami, R. and Jafarpour, V. 2019. Experimental Study of Residual Stresses Due to Inconel X-750 Creep-feed Grinding by the Electropolishing Layer Removal Technique. 4: 65-71

[26] Dreiera, S. and Denkenaa, B. 2014. Determination of Residual Stresses in Plate Material by Layer Eemoval with Machine-integrated Measurement. Procedia CIRP. 24: 103 – 107.

[27] Kruszyński, B., Togo, S. and Wójcik, R. 2003. Possibility to Control Surface Integrity in Grinding. Journal of Manufacturing Science and Technology. 4(1): 22-27.

[28] Gadalińska, E. and Wronicz, W. 2016, Electropolishing Procedure Dedicated to In-depth Stress Measurements with X-ray Diffractometry. Fatigue of Aircraft Structures. 1: 65-72.

[29] Han, W. and Fang, F. 2019. Fundamental Aspects and Recent Developments in Electro Polishing. International Journal of Machine Tools and Manufacture. 139: 1-23.